Article

The Role of a Permeable Sand Column in Modifying Tidal Creek Nutrient Inputs into the Coastal Ocean

Nicholas A. Legut [1,2], Brandon T. Hawkins [1] and Angelos K. Hannides [1,*]

[1] Department of Marine Science, Coastal Carolina University, Conway, SC 29528-6054, USA; nalegut@coastal.edu (N.A.L.); bthawkins@coastal.edu (B.T.H.)

[2] Illinois State Geological Survey, Prairie Research Institute, University of Illinois at Urbana-Champaign, 615 E. Peabody, Champaign, IL 61820, USA

* Correspondence: ahannides@coastal.edu; Tel.: +1-843-349-2538

Abstract: Estuarine tidal creeks are an important conduit for freshwater run-off into the coastal ocean. In Long Bay, South Carolina, tidal creeks terminate in swashes—broad sandy fields constantly reworked by discharged creek water. We examined the role of a highly permeable sandy column in altering the nutrient loading of the passing water at Singleton Swash, Myrtle Beach, South Carolina. Seasonal transects along the swash's primary channel documented gradients in physical and biogeochemical parameters. The nutrient and chlorophyll *a* concentrations were higher in the sediment than in the overlying water, consistent with coastal sediments as a major site of organic matter degradation, nutrient regeneration, and benthic primary productivity. Oxygen, nutrient, and chlorophyll concentrations exhibited a strong seasonal component, explained by a photosynthesis–respiration balance shift between summer and winter. The conservative mixing model approach to elucidate the sink–source patterns was moderately informative due to the lack of a gradual salinity gradient from land to ocean, due to substantial tidal flushing and observable nutrient-rich surface freshwater discharges along the channel that fueled substantial submerged aquatic macroalgal growth. Future studies should focus on the role of benthic photosynthesizers, both microbial and macroalgal, in retaining land-derived nutrients in irrigation freshwater inputs prior to them reaching the coastal ocean.

Keywords: permeable sediments; swashes; tidal creeks; nutrients; chlorophyll; benthic primary productivity; conservative mixing

1. Introduction

Populations in coastal regions of the U.S. are continuously expanding at a rate of almost 10% every ten years [1]. As land-use changes to accommodate growth, increase in impervious surfaces [2] and nutrient-rich freshwater discharges [3] result in a more rapid delivery of nutrients into estuarine and coastal waters. In shallow marine environments, excess nutrient input can result in the eutrophication of the water column and, in severe cases, hypoxic conditions may develop [3]. These anthropogenic stressors can ultimately alter the condition of the water-column and benthic habitats and may lead, for instance, to harmful algal blooms [3] and the displacement of stress-sensitive macrobenthic taxa by stress-tolerant ones [4]. It is therefore important to investigate the nexus of coastal land-use change, nutrient loading, and nutrient discharge processes to better understand land-derived nutrient discharges into coastal water bodies.

Estuarine tidal creeks are one of many conduits for freshwater run-off into the coastal ocean and frequently intersect the sandy beaches that line the land–ocean interface [5,6]. As tidal creeks reach these broad sandy beaches, the flowing water interacts with the nearshore sediment transport

processes to form transient meandering swashes [6,7]. An extensive investigation of tidal creeks ending in swashes in the Grand Strand region of South Carolina [5] concluded that a portion of land-derived materials were retained in their respective watershed prior to arrival to the swashes and discharge into the coastal ocean.

The biogeochemical characteristics and function of the sandy terminus of estuarine tidal creeks are not fully understood, but should be evaluated in order to fully assess the role of freshwater discharges through swashes on the biogeochemistry of the coastal ocean [5,8]. A key driver of sandy column function is its high permeability, which results in rapid filtration of organic matter, nutrient regeneration, and primary productivity as the regenerated nutrients are transported rapidly to the sediment surface and overlying water column [9–12]. The implications of this rapid cycling exchange on biogeochemistry and ecology have been studied extensively over a variety of spatial and temporal scales [13–15]. In swashes, where physical transport is present and the water column is shallow, transformations of organic materials by microbial respiration are likely to occur in the sediment rather than the water column [16]. Sedimentary respiration (left-to-right direction in Equation (1), based on [17]), using Redfield–Richards stoichiometry) releases dissolved inorganic nutrients into the pore-water where they may be subject to physical transport:

$$(CH_2O)_{106}(NH_3)_{16}(H_3PO_4) + 138O_2 \leftrightarrow 106CO_2 + 16HNO_3 + H_3PO_4 + 122H_2O \qquad (1)$$

Without any further transformations, these dissolved inorganic nutrients would be circulated back into the water column by advective pore-water flows [9]. However, highly abundant biofilms of microphytobenthic communities, on the order of millions of cells per cubic centimeter, are able to develop in the top 5 mm (mm) of the photic permeable sediments [18]. These biofilms may assimilate dissolved inorganic nutrients derived from the sedimentary nutrient pool during photosynthesis (right-to-left direction in Equation (1)), acting as a living nutrient filter [19,20], and may have the potential to greatly influence the nutrient dynamics in swashes.

Our study examines the swash sediment and water biogeochemical properties in view of sediment–water interaction, seasonality and freshwater inputs from a heavily modified urban watershed. A high-resolution transect was sampled throughout the swash's primary channel across five sampling dates to identify changes in a suite of water-column and sedimentary parameters with particular attention to the function of the underlying permeable sand column. The chemical and biological change in the concentrations of the various dissolved nutrients and particulate materials in the overlying water and in the sediment along the transect is supplemented by assessing the non-conservative behavior of these nutrients and materials, both in space (along the transect) and in time (seasonally). Our study fundamentally explores how a living, highly-permeable medium, such as a sandy beach, may interact with and modify the biogeochemical composition of surface runoff entering the coastal ocean.

2. Materials and Methods

2.1. Study Site

Singleton Swash in Myrtle Beach, South Carolina, was selected as the study site for numerous reasons. It drains the third largest watershed (613 hectares) of 15 swashes in the Grand Strand of South Carolina [5]. Impervious surfaces, high-to-moderate development and low development cover 26%, 19% and 22% of the watershed area, respectively [5]. Tourist and recreational infrastructure abound (e.g., Figure 1) and may exert significant pressure on water quality, for instance due to fertilizer application on golf concourses and landscaping, while the erosional threat posed by the swash on this infrastructure necessitates the management of the swash by Horry County, South Carolina, through periodic dredging and redirection of the primary channel [21]. As a result, this swash has been monitored and studied for several years using a variety of methods and approaches [22–25], providing useful background and continuity. A primary tidal channel cuts through the sandy terminus of Singleton Swash (centered at 33°45.394′ N, 78°47.669′ W) and constantly reworks a sandy intertidal

flat, resulting in a dynamic morphology (Figure 1) [21,22]. During our study period (2017–2019), a tidal pool of stagnant water remained disconnected from the primary channel at low tide.

Figure 1. Study site and stations in Long Bay, South Carolina (satellite image courtesy Google Earth, February 2019). The yellow line indicates the primary channel transect that is anchored by a fixed landward-most station (Station 10, yellow triangle) and the oceanward-most station (Station 1 or SSC, yellow circle), which was determined on the day of sampling given the track of the primary channel. Transect stations 2–9 were spaced 30–50 m apart along the transect. The Singleton Swash Beach CCU sand biogeochemistry monitoring station is indicated by SSB.

Long Bay (South Carolina), in which the primary channel empties, is a shallow mesotidal mixed-energy, open-ocean embayment that is subject to diffuse discharges from multiple creeks and inlets like Singleton Swash [8]. Climatological characteristics for the duration of the study period are shown in Figure 2. Atmospheric temperature and daylight duration show typical seasonal variation, while precipitation records document several intense rainfall events, especially the one associated with Hurricane Florence in September 2018. The effect of this event is noticeable in the below-normal coastal-ocean salinities documented at a nearby pier monitoring station (Figure 2).
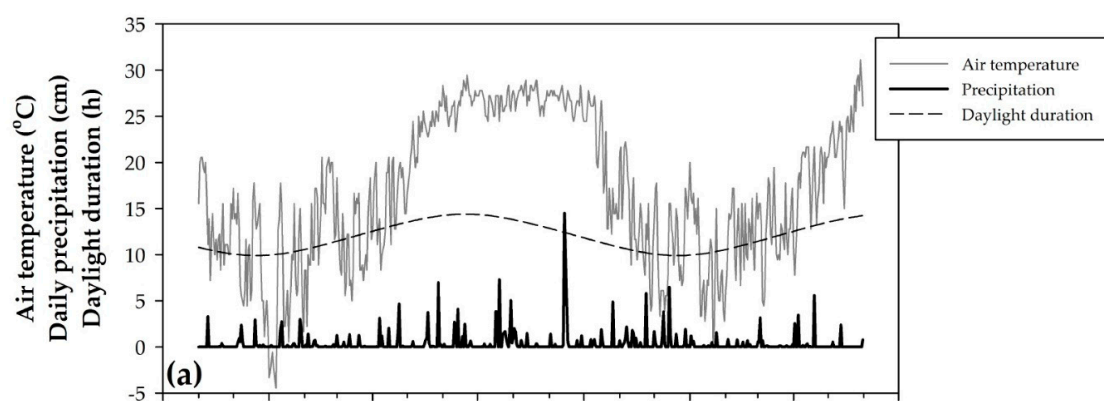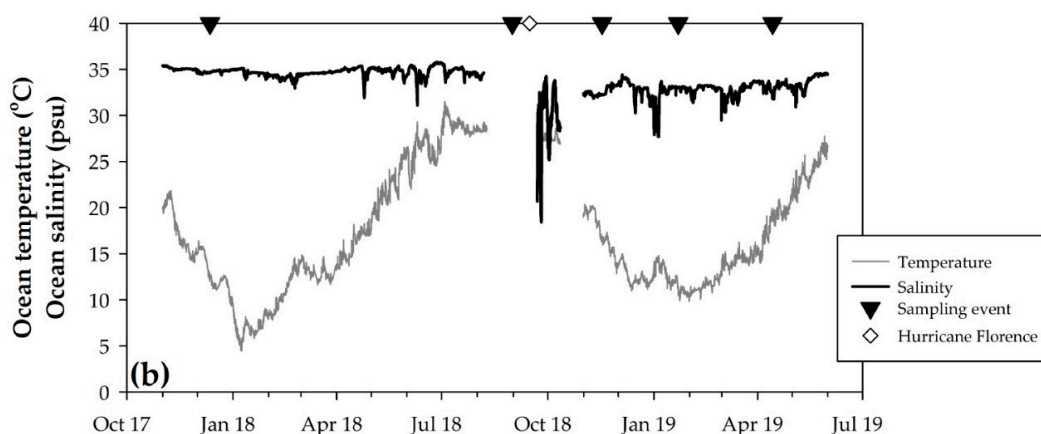

Figure 2. *Cont.*

Figure 2. (**a**) Atmospheric temperature and precipitation for the National Weather Service station KCRE, North Myrtle Beach Grand Strand Airport, 33°49.002′ N, 78°43.002′ W (https://w2.weather.gov/climate/index.php?wfo=ilm) and daylight duration estimated from sunrise and sunset times from the US Naval Observatory (https://aa.usno.navy.mil/data/docs/RS_OneDay.php). (**b**) Coastal oceanic data collected from the bottom sensors (5.5 m depth) of the Apache Pier station, 33°45.690′ N, 78°46.788′ W (http://bccmws.coastal.edu/lbos/). Sampling event dates are shown in black circles and the timepoint of Hurricane Florence's passage is shown by the white triangle.

2.2. Sampling Approach

Based on results from preliminary sampling along a five-station transect on 12 December 2017, we decided to time our sampling to coincide with the low tide when the influence of land-derived water and its characteristics is most pronounced, given the possibility that the freshest water would not necessarily be observed at the landward-most station.

On 29 August 2018, we collected pore-water and solid-phase property profiles down to 90 cm from a periodically monitored beach station in the low-tide swash zone, indicated as SSB (Singleton Swash Beach, 33°45.368′ N, 78°47.525′ W) in Figure 1, and from the location of the creek's discharge to the ocean. The purpose of this sampling was to guide our sedimentary sampling approach within the primary channel, by indicating the depth in the sediment column at which the nutrient concentrations are substantially elevated relative to the water column.

Sampling of the primary channel took place across seasons to capture any seasonal fluctuations due to light and temperature variation.

The primary channel was sampled along a 10-station transect on four dates: 31 August 2018; 17 November 2018; 22 January 2019; and 14 April 2019. Every sampling event started at the oceanward-most station 1 (also designated SSC, shown as a yellow circle) at the location where the primary channel emptied into the swash zone on each specific date. An additional nine stations spaced 30–50 m apart were sampled along the primary channel (shown as a yellow line in Figure 1) and always ending at the landward-most station 10 (33°45.453′ N, 78°47.669′ W, shown as a yellow triangle in Figure 1) where the marsh tidal creek enters the swash's sandy terminus.

The tidal pool (33°45.412′ N, 78°47.633′ W) and a marsh creek station (33°45.512′ N, 78°47.581′ W), approximately 200 m upstream from the landward-most station of the primary channel transect (Figure 1), may be characterized by lower rates of solute exchange between the overlying water and the sand column than the primary channel for different reasons. The tidal pool sediment column appeared to be sandy and therefore highly permeable but water flow is low to non-existent. Marsh creek sediment underlies the flowing water but may consist of fine sand and mud of lower permeability. Both of these settings were sampled to explore the role of sedimentary permeability in shaping the biogeochemical characteristics.

Finally, in January and April 2019, we observed surface discharges from the embankment along a protective metal bulkhead shielding an adjacent property (the zone is marked with a red line in Figure 1) and sampled this water for determination of salinity, oxygen, and nutrient concentrations.

2.3. Field Measurements and Sample Collection

Prior to sampling the overlying water, a YSI ProDSS meter with an ODO/CT probe assembly (YSI Inc., Yellow Springs, OH, USA) was used to record the station's GPS location, water temperature, salinity, and O_2, while turbidity was measured using a HACH 2000Q portable turbidimeter (Hach, Loveland, CO, USA).

The overlying water (OW) samples were retrieved using 10-mL polypropylene-polyethylene syringes and filtered on site through 0.2-μm, nylon-membrane in-line filters into 7-mL scintillation vials for inorganic nutrient analyses. Additional water samples for chlorophyll *a* (Chl *a*) analysis were collected in 125-mL HDPE bottles.

The surface sediment (0–10 cm) samples for laboratory analysis of the grain-size distribution and permeability were collected using 60-mL cut-off syringes, and the sedimentary (Sed) Chl *a* samples were collected from 0–5 cm (see Section 3.2 below) using 10-mL cut-off syringes and transferred to pre-weighed glass vials. The August 2018 sedimentary cores at SSB and the creek discharge station (SSC) were obtained using an Icelandic piston corer (Aquatic Research Instruments, Hope, ID, USA). The cores were sliced in the lab at 10-cm intervals and subsampled for permeability, grain size analysis, Chl *a*, and loss-on-ignition at 550 °C (LOI_{550}) as a proxy for organic matter content.

Pore-water (PW) samples were retrieved using an MHE PushPoint sampler (MHE Products, East Tawas, MI, USA). Based on the August 2018 profiling data, PW sampling at all stations in the primary channel took place at 30 cm below the sediment–water interface (see Section 3.2 below).

All samples were immediately stored on ice in a cooler for transportation to the laboratory, where they were either processed immediately or frozen until analysis.

2.4. Analytical Methods

Permeability was determined by the constant-head method [26,27]. Grain size distribution was determined by wet sieving and the mean grain size (mm, phi), median grain size (mm, phi), sorting (phi), and skewness (dimensionless) were determined by the statistical definitions in [28].

Chl *a* was measured by fluorescence after extraction in acetone, as described in [29]. Sedimentary samples were processed according to [30]. The LOI_{550} was determined according to [31].

The methods used for nutrient analyses in this study have been modified to accommodate small sample volumes (1–1.2 mL). A microvolume column was set up for the reduction of nitrate (NO_3^-) to nitrite (NO_2^-), according to the principles in [32], and nitrite was analyzed spectrophotometrically [33], with limits of detection of 0.37 and 0.02 μmol L^{-1} for nitrate and nitrite, respectively. Ammonium (NH_4^+) was analyzed by fluorescence according to [34], with a limit of detection of 0.17 μmol L^{-1}. The dissolved inorganic nitrogen (DIN) concentration was calculated as the sum of the concentrations of nitrate, nitrite, and ammonium. Phosphate (PO_4^{3-}) was analyzed spectrophotometrically by the molybdenum blue complexation method with a limit of detection at 0.26 μmol L^{-1} [35,36].

2.5. Data Analysis

Data were explored graphically using SigmaPlot (Systat) and statistically using SPSS (IBM) by suitable statistical methods [37]. Property–property plots, including the salinity vs. concentration plots used in the conservative mixing analysis, were generated using the averages (and standard deviations) of each property at each station on each sampling date. One-way ANOVA was used to determine if significant differences in the concentrations of O_2, nutrients, and Chl *a* existed between seasons as well as between the sedimentary and overlying water environments (significance level of 0.01).

Linear conservative mixing models [38] were developed by fitting a linear regression model through the two salinity end-member (x-axis) vs. chemical concentration (y-axis) pairs in the primary

tidal channel on each sampling event, yielding a model slope (m_{Model}) and a model intercept (b_{Model}). Deviation from conservative mixing, ΔC (otherwise known as the residual value), was quantified as follows:

$$\Delta C = C_{Meas} - C_{Model} \tag{2}$$

where C can be replaced by the formula or notation of the compound under investigation, C_{Meas} is the measured concentration at non-end-member stations, and C_{Model} is the theoretical concentration predicted by the linear conservative mixing model, as follows:

$$C_{Model} = m_{Model} \times Sal_{Meas} + b_{Model} \tag{3}$$

where Sal_{Meas} is the measured salinity at a non-end-member station, m is the slope of the linear model and b is the intercept of the linear model.

Deviations from conservative behavior for each property were evaluated by constructing box-and-whisker plots of the residual values throughout the swash for each property on each sampling event. The assessment of non-conservative behavior for a measured property was determined by the position of the 25–75% interquartile range relative to zero. Positive and negative residuals indicated source and sink behavior, respectively. Source/sink behavior was also examined across seasons and properties to determine shifts in the balance between photosynthesis and respiration.

3. Results

3.1. Sedimentary Geological and Physical Properties

The sedimentary and physical properties across the study site are summarized in Table 1 and Figure 3. Overall, the sediment on the shore and along the primary channel is classified as moderately sorted medium sand with symmetrical skewness and a high permeability ($>10^{-12}$ m^2). Permeability is substantially lower in the relatively quiescent sandy tidal pool and is lowest in the marsh creek.

Table 1. Sedimentary geological and physical properties of the three sedimentary settings sampled during this study (mean ± 1 standard deviation). The classification for sorting and skewness is based on McManus (1988).

| Property	Primary Channel ($n = 35$)	Tidal Pool ($n = 3$)	Marsh Creek ($n = 3$)
Permeability (m^2)	$2.9 \times 10^{-11} \pm 9.4 \times 10^{-12}$	$3.1 \times 10^{-12} \pm 2.0 \times 10^{-12}$	$1.9 \times 10^{-12} \pm 8.0 \times 10^{-13}$
Porosity	0.44 ± 0.02	0.45 ± 0.01	0.46 ± 0.00
Mean grain size (phi)	1.87 ± 0.37	2.3 ± 0.3	2.3 ± 0.4
Mean grain size (µm)	282 ± 61	208 ± 45	208 ± 49
Median grain size (phi)	1.85 ± 0.36	2.2 ± 0.2	2.3 ± 0.2
Median grain size (µm)	285 ± 62	216 ± 30	209 ± 33
Fines (<63 µm) fraction (%)	0.2 ± 0.4	1.9 ± 1.6	1.3 ± 1.4
Sorting, σ_1	0.73 ± 0.13	0.76 ± 0.03	0.70 ± 0.02
Sorting, classification	Moderately sorted	Moderately sorted	Moderately sorted
Skewness, SK_1	-0.05 ± 0.13	-0.13 ± 0.19	-0.13 ± 0.28
Skewness, classification	Symmetrical	Negatively skewed	Negatively skewed
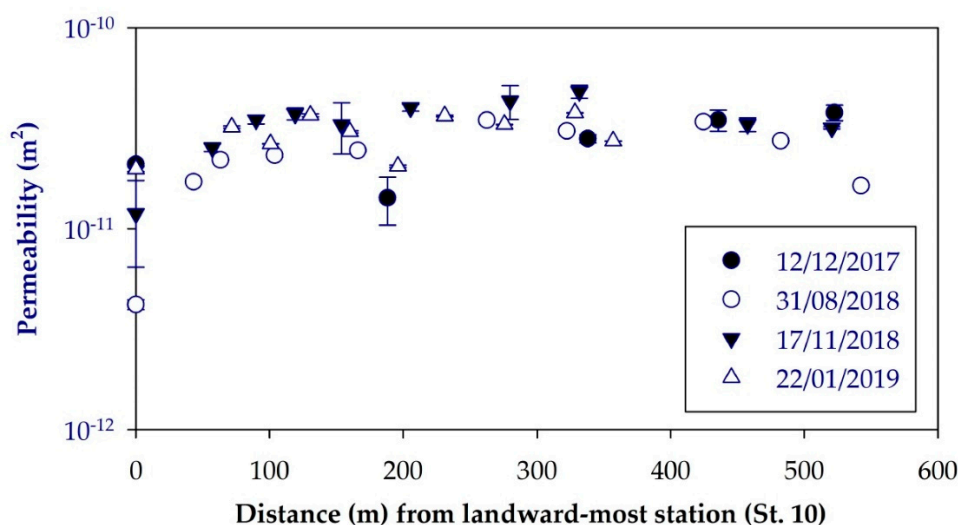
Figure 3. Surface (0–10 cm) sand permeability along the primary channel.

3.2. Sedimentary Biogeochemical Profiles

The pore-water nitrate and phosphate and solid-phase Chl *a* profiles are shown in Figure 4. Nutrient concentrations gradually build up with depth and attain high values by 30–45 cm below the sediment–water interface (SWI). Chl *a* is highest at 0–20 cm and gradually decreases with depth. Based on these profiles, the swash sampling protocol was adjusted so that the pore-water samples were obtained from 30 cm below the SWI and sedimentary Chl *a* samples were collected from the top 5 cm.
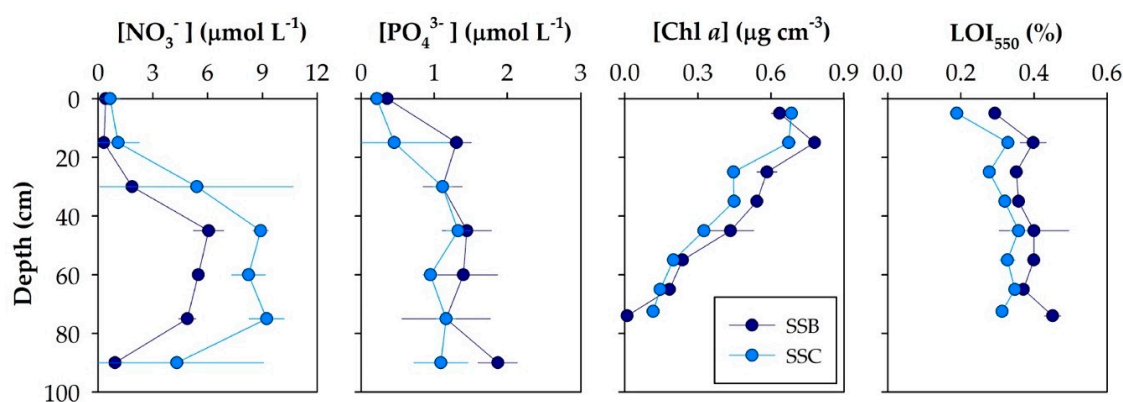
Figure 4. Pore-water nitrate and phosphate and solid-phase Chl *a* and loss-on-ignition at 550 °C (LOI$_{550}$) profiles collected from the Singleton Swash beach monitoring station (SSB) and the location of the creek's discharge into the ocean (SSC) on 29 August 2018.

3.3. Primary Channel Transect Patterns

Table 2 indicates the transect distances, salinity and temperature values, and the distance at which the minimum salinity was detected on the five sampling events.

Table 2. The primary channel transects' sampling details, water characteristics (salinity, temperature, and distance at which the minimum salinity was detected), and daylight duration. Transect distance is measured with the landward-most station at 0 m (orange star in Figure 1). PSU: practical salinity units.

Property	12/12/2017	21/08/2018	17/11/2018	22/01/2019	14/04/2019
Total transect distance (m)	522	543	521	357	411
Number of stations	5	10	10	10	10
Distance of minimum salinity	436	322	0	357	0
Salinity (PSU, mean ± 1 s.d.)	28.9 ± 1.7	32.9 ± 0.8	11.4 ± 7.2	31.6 ± 0.4	27.7 ± 1.5
Temperature (°C, mean ± 1 s.d.)	10.0 ± 0.7	31.0 ± 0.4	12.4 ± 1.5	10.6 ± 0.2	22.7 ± 0.7
Daylight duration (h)	9.95	12.9	10.35	10.32	12.98

Biogeochemical data from the overlying water and sediment of the primary channel from the five sampling events are shown as conservative mixing plots in Figure 5 and as box-and-whisker plots of absolute concentration values and residuals (ΔC, Equation (2)) in Figure 6.
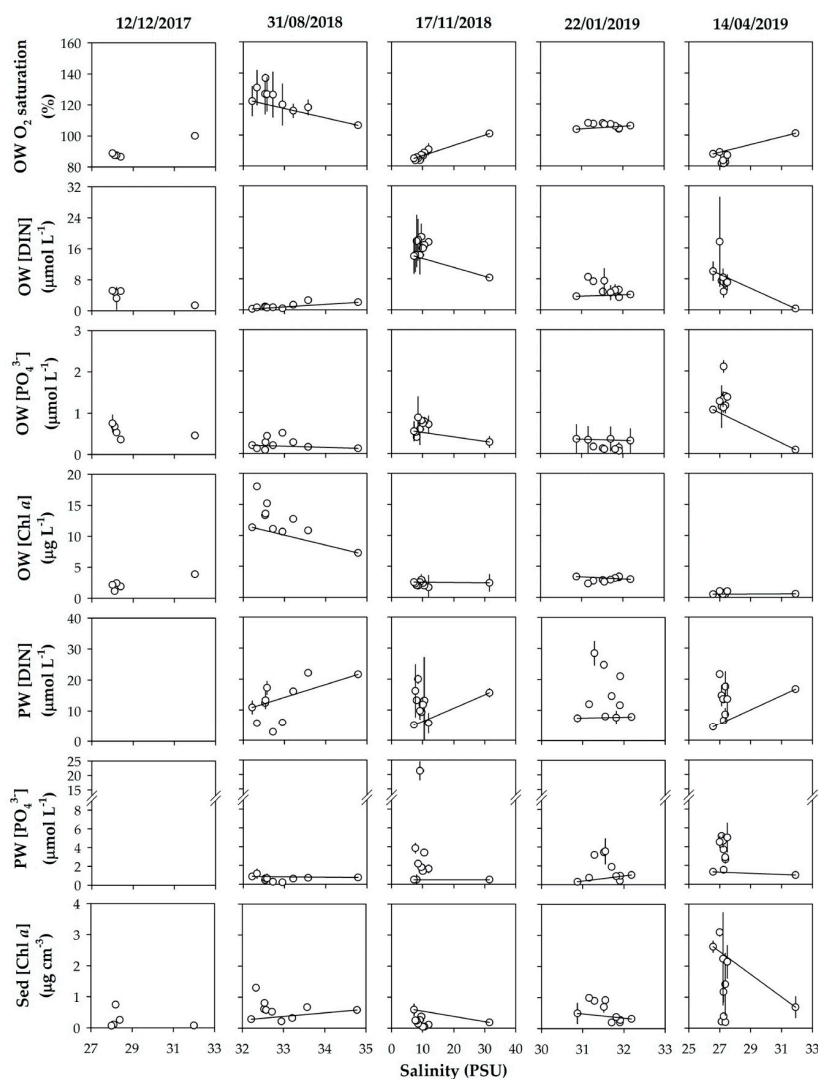

Figure 5. Conservative mixing plots of properties measured in the overlying water (OW), pore-water (PW), and sedimentary solid phase (Sed) along the primary channel during the five transect sampling events. Straight lines indicate conservative mixing lines, which were not included in the case of 12 December 2017, given that only five stations were sampled, as opposed to 10 stations on all other dates.
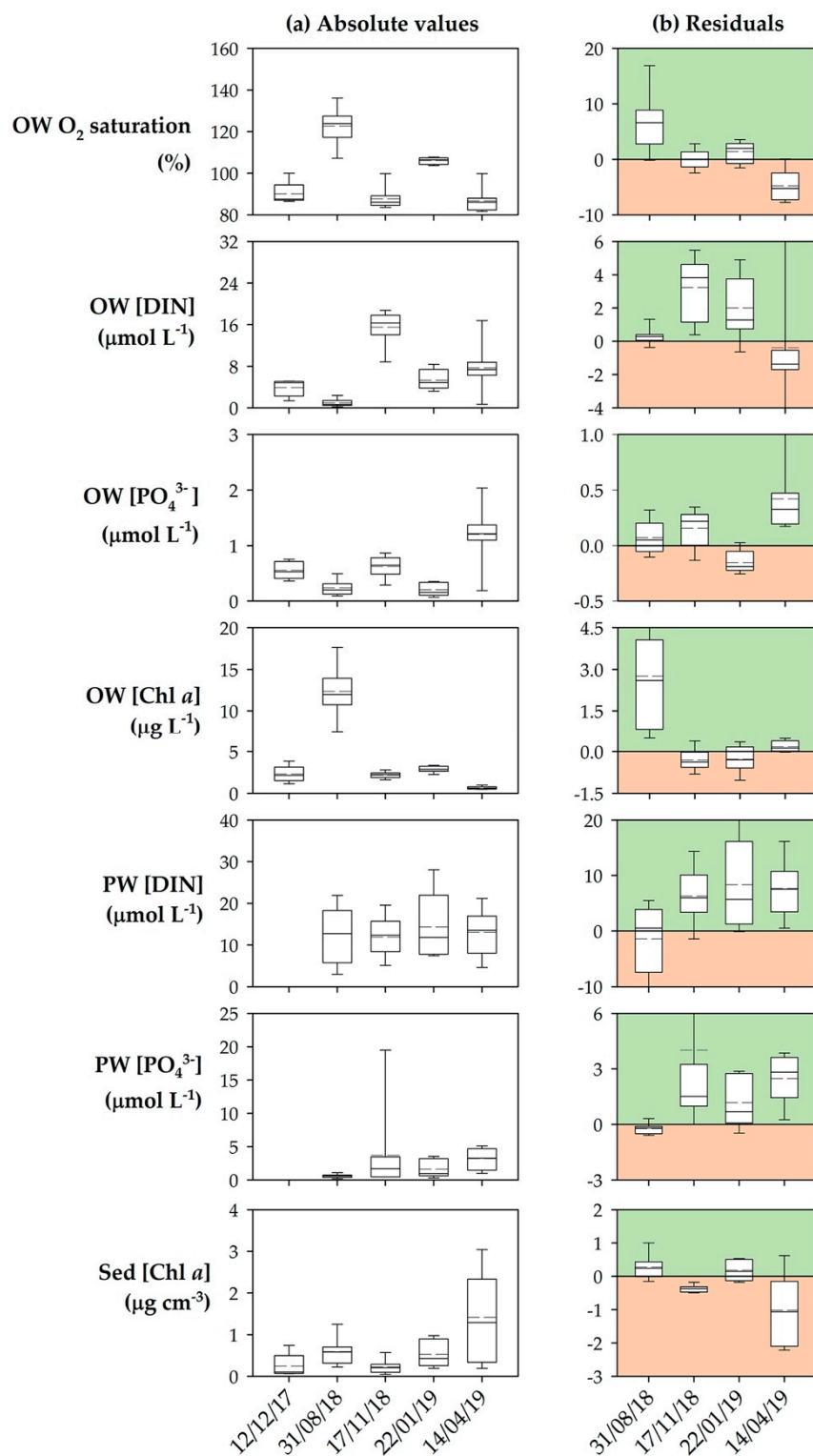
Figure 6. Box-and-whisker plots of (**a**) the absolute concentration values and (**b**) the concentration residuals on the five transect sampling events. Boxes indicate the 25 to 75 percentiles about the median (shown by a straight line; mean indicated by a dashed line) while whiskers indicate the 5 to 95 percentiles. Data from 12 December 2017 were not included in the conservative-mixing analysis given that only five stations were sampled, as opposed to 10 stations on all other dates.

Statistically significant differences were detected between the sampling events in all water-column properties and sedimentary Chl *a* ($p < 0.01$), but no such differences were present in the remaining sedimentary properties (PW DIN, $p = 0.851$; PW PO_4^{3-}, $p = 0.151$).

Sedimentary vs. overlying water concentrations of Chl *a*, DIN, and PO_4^{3-} in the primary swash channel on the main sampling dates are shown in Figure 7. The sedimentary concentrations are higher than the overlying water concentrations ($p < 0.01$) on all occasions, with the exception of inorganic nutrients on 17 November 2018 (DIN, $p = 0.056$; PO_4^{3-}, $p = 0.140$) and DIN on 14 April 2019 ($p = 0.024$). The primary channel sedimentary LOI_{550} values on 31 August 2018 were $0.69 \pm 0.53\%$.
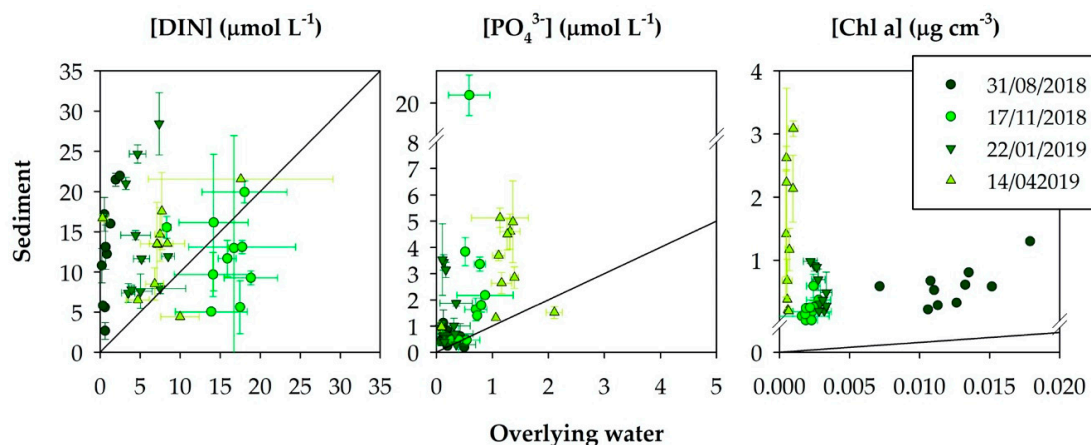

Figure 7. Comparison of the overlying water (*x*-axis) and sedimentary (*y*-axis) concentrations of DIN, PO_4^{3-}, and Chl *a* at all primary channel stations recorded during the 10-station sampling events. The solid line indicates a 1:1 analogy.

3.4. Comparison with Auxiliary Stations

The auxiliary stations, such as the marsh channel and a sandy tidal pool flushed at high tide, represent a contrast to the primary swash channel as settings of lower solute exchange between the water column and sediments (see Section 2.2). Sedimentary physical and geological properties at the three stations and sampling events are compared in Table 1, while pore-water DIN and phosphate and sedimentary Chl *a* are shown in Figure 8. The three settings exhibited values at similar magnitudes ($p > 0.01$) on all dates, with the exception of sedimentary Chl *a* on 22 January 2019 and 14 April 2019. Post-hoc analysis (Student–Neuman–Keuls) indicated that the primary channel had statistically lower values than the other settings on 22 January 2019, and the marsh creek setting on 14 April 2019. On 31 August 2018, we also determined sedimentary LOI_{550} in the tidal pool at 0.89%, as compared to $0.69 \pm 0.53\%$ in the primary channel stations.
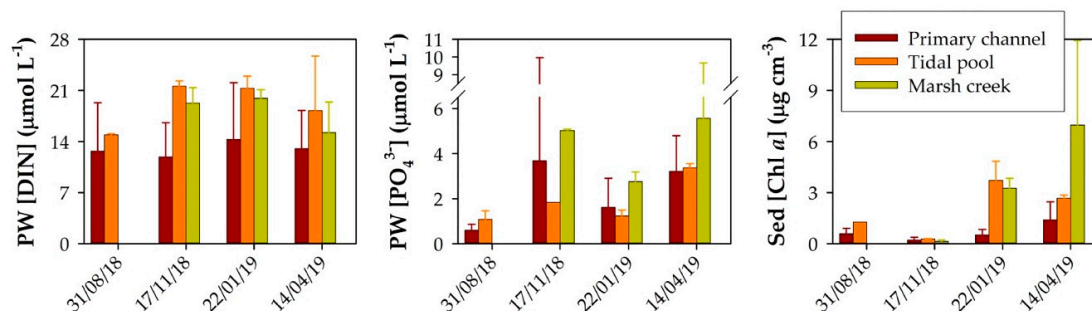

Figure 8. Comparison of pore-water (PW) dissolved inorganic nitrogen (DIN), phosphate (PO_4^{3-}), and sedimentary (Sed) Chl *a* at the three sedimentary settings on the four 10-station sampling events. Absent columns indicate no sampling/analysis.

In addition to these stations, we sampled and analyzed water from the surface point discharges observed on 22 January 2019 and 14 April 2019 (see Section 2.2). A comparison of salinity, O_2% saturation, dissolved inorganic nitrogen (DIN), and phosphate (PO_4^{3-}) in the primary channel and point discharges on those two dates is shown in Figure 9. Water from the surface discharges was nearly fresh, with a salinity of 1.4 ± 1.1 PSU (practical salinity units), and nutrient-enriched compared to primary channel water. Primary channel vs. point discharge values are statistically significantly different ($p < 0.01$) on all dates and for all properties, with the exception of O_2 saturation on 14 April 2019 ($p = 0.243$).
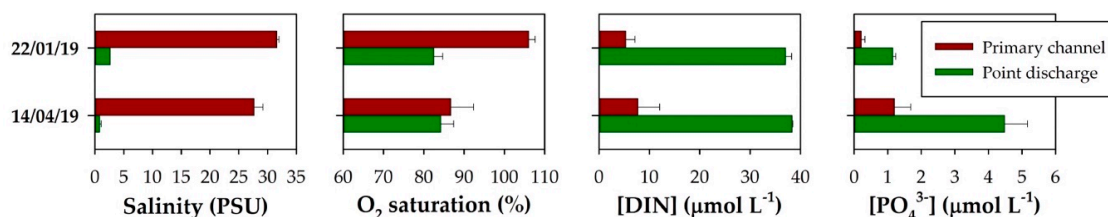

Figure 9. Comparison of salinity, O_2% saturation, dissolved inorganic nitrogen (DIN), and phosphate (PO_4^{3-}) in primary channel stations and point discharges during the two sampling events when these discharges were present. Primary channel DIN and PO_4^{3-} are overlying water values.

4. Discussion

4.1. The Sedimentary Environment as a Benthic Nutrient Filter

The primary channel of Singleton Swash is composed of highly permeable, medium sand (Figure 5). In contrast, sediment in the sandy tidal pool and marsh tidal creek consists of finer sand than the primary channel and, consequently, permeabilities that are lower by 6 and 20 times, respectively, due to larger fractions of fine-grained sediments (grain diameter < 63 μm) than the primary channel sand (Table 2).

Sedimentary concentrations of DIN, PO_4^{3-}, and Chl *a* are higher than the overlying water values on most instances during the study period (Figure 7). The pattern is consistent with the role of coastal sediments as a major site of organic matter degradation and nutrient regeneration, with an accompanying flux of nutrients from a region of high concentration, the sand column, to a region of low concentration, the water column. High sedimentary Chl *a* concentrations at the SWI are characteristic of the "benthic nutrient filter" effect, whereby sediment surface microphytobenthos intercept sedimentary nutrients before they reach the overlying water [19]. Future exploration of this effect should include a more robust investigation of both carbon and nitrogen cycling, as well as microbial activity as indicated in [19]. We were only able to determine LOI_{550} as a proxy of organic matter content in August 2018 during this study, both in beach (swash zone) profiles (0.34 ± 0.06%, Figure 4) and across the primary channel transect (0.69 ± 0.53%), and these results indicate the importance of organic matter enrichment within the swash terminus and the necessity to study this further in both sediments and overlying water.

While the direct exchange of matter across this highly permeable SWI was not measured, the rapid water currents and uneven bathymetry combined with a highly permeable sedimentary column likely result in exchange of particulate and dissolved materials across the primary channel SWI via turbulent forces [12,39]. We compared porewater nutrients and sedimentary chlorophyll on four separate sampling events between the primary channel on the one hand and the tidal pool and marsh creek on the other, where the sediment–water column exchange may not be as rapid as in the primary channel (see Section 2.2). We did not detect significant differences between the three settings in most cases, with the only exception being sedimentary Chl *a* on 22 January 2019 and 14 April 2019, when the primary channel had significantly lower concentrations than both other settings and the marsh creek, respectively. The establishment of a biofilm in less turbulent conditions than those of a rapidly moving

sand field, as is the case in the primary channel, may explain the higher Chl *a* build-up on these two dates and the fine-scale profiles of the Chl *a*; carbohydrate content, a common microbial biofilm indicator [40], may help illuminate this distinction further in future studies.

4.2. Seasonality

The primary channel exhibits biogeochemical conditions that are expected of swashes in the Grand Strand region with overlying water DIN, PO_4^{3-}, and Chl *a* concentrations similar to those in the discharge waters of Withers Swash [5]. With the exception of sedimentary DIN, all other sedimentary and overlying water biogeochemical properties vary with the seasons, as predicted by shifts in balance between photosynthesis and respiration (Equation (1)) driven by light availability and, to a lesser extent, temperature fluctuations (Figure 10).
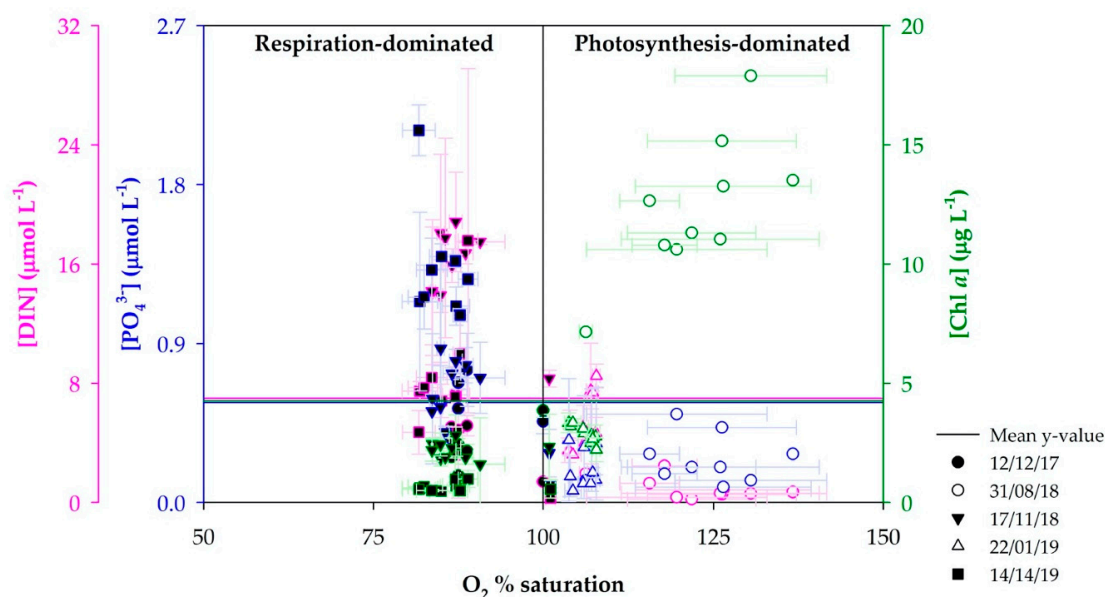

Figure 10. Overlying water concentrations of DIN, PO_4^{3-}, and Chl *a* on the main sampling dates are shown in relation to O_2 saturation. The vertical black line indicates 100% O_2 saturation. The horizontal colored lines indicate the mean values of the concentrations blotted on the vertical axes.

Based on ongoing time-series monitoring of Long Bay beaches, sandy sediments experience annual minimum Chl *a* concentrations in October–November, a major maximum period in June–August, and a minor one ("spring bloom") in February–March (A.K.H., unpublished data). Data from this study are in accordance with this pattern: Chl *a* and O_2 are elevated and nutrient concentrations suppressed on 31 August 2018 and 22 January 2019, with the inverse observed on 12 December 2017, and 17 November 2018 (Figure 10). The data from April 2019, however, are inconsistent with this pattern. Overlying water is undersaturated with respect to O_2 and high in nutrients, compared to 22 January 2019. We explore this difference in view of nutrient-rich freshwater inputs from surrounding developments in the next section.

4.3. Source–Sink Behavior and Modification of Land-Derived Nutrients

The results of the conservative mixing analysis indicate that monitored properties exhibit non-conservative behavior for most of the study period (Figure 6). Pore-water nutrients exhibit source behavior in all seasons except August (a net balance between source and sink), a finding consistent with the role of sandy sediments as a biofilter, whereby overlying water organic matter is filtered and respired to generate inorganic nutrients [11].

The fate of the generated inorganic nutrients is seasonally dependent, as this study's conservative mixing analysis reflects these general patterns (Figure 6). The swash is a source for O_2 and both overlying and Sed Chl *a* during the peak-Chl *a* period in this region (August), while in the low-Chl *a* period (November/December) it is a sink for Chl *a* and a source for nutrients. By January, we would expect to see the source–sink behavior to revert to conditions representative of higher Chl *a*, i.e., higher primary productivity. However, the data from January and especially April 2019 are equivocal: on 14 April 2019, the overlying water of the primary channel constitutes a source for Chl *a* but a sink for O_2, and different trends for DIN and phosphate, while Sed Chl *a* exhibits sink behavior while we would expect the latter (Figure 6).

This exception may be related to input of freshwater from surface run-off flowing into the middle of the primary channel transect from adjacent lawns at relatively high rates. We observed, sampled, and analyzed surface run-off in both January and April 2019, and we note, by observation, that both the flow rate and occurrence of surface discharges were much higher in April and they coincided with substantial submerged macroalgal overgrowth on hard substrates on the banks of the primary channel (Figure 1). Respiration of this overgrowth would result in O_2 draw-down and a concomitant increase in denitrification rates that would selectively remove nitrate (hence, DIN) but not phosphate from the system, thus explaining both the patterns in overall concentrations and sink–source behavior.

The conservative mixing approach, commonly applied in the case of large estuaries [38], could be perceived as appropriate in the case of a swash primary channel for numerous reasons. The landward station is rarely characterized by the freshest water (Table 2), with freshwater entering the swash at surface discharges or potentially through groundwater seepage throughout the tidal cycle. Moreover, salinity gradients along the primary channel are further muted by stronger flood currents than ebb currents that rapidly mix an accumulating water mass within the marsh tidal creek and emptying out during low tide [25]. Tidal- or diurnal-period processes are nested within seasonal or annual processes. For instance, human practices, especially daily irrigation and fertilizer application, vary seasonally and will impact the supply of freshwater and nutrient loads to the swash and coastal zone. In addition, high-precipitation events will recharge upland watersheds that will drive substantial freshwater discharges to the coastal ocean. Specifically, the low salinities observed in the primary channel on 17 November 2018 are a probable consequence of Hurricane Florence-induced flooding still occurring as the saturated Pee Dee Basin slowly discharged waters downstream to the lower floodplains (see [41] for analysis of Waccamaw River gauge data).

The effort to synthesize all the data from our study and, consequently, to capture the full range of salinities we documented and their concomitant oxygen and nutrient concentrations, is shown in Figure 11. The plotted trends indicate that direct freshwater inputs and oceanic end-members across our sampling events capture anticipated theoretical end-member features. The data from the remaining primary channel stations fail to align on these conservative mixing models in a manner consistent with the fundamental seasonal shift between photosynthesis and respiration (Equation (1)), an outcome which is in agreement with our sink–source analysis already discussed in this section.
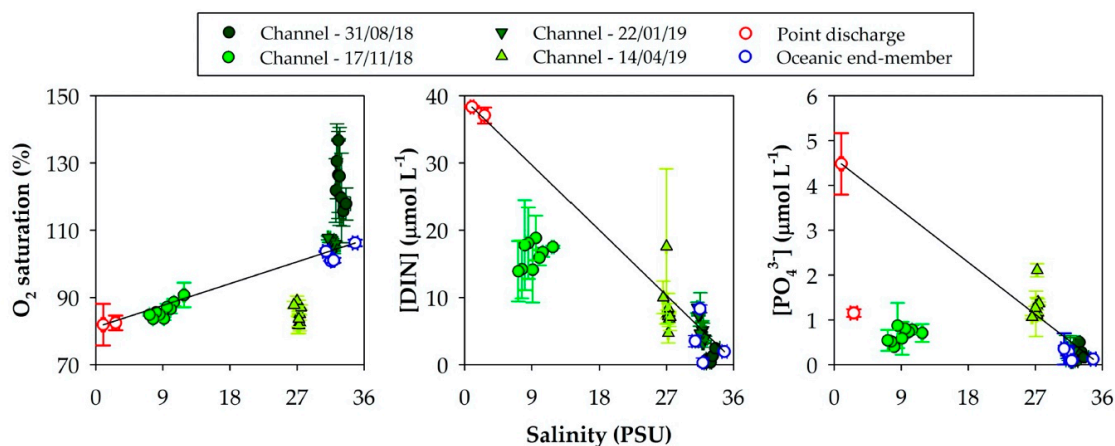
Figure 11. Composite conservative mixing curves for oxygen saturation, DIN, and phosphate during the study period using data from the primary channel and the surface discharges. Oceanic end-members from the four main sampling events are plotted as blue circles and surface discharges from January and April 2019 are plotted as red circles.

Therefore, while the exploration of concentration changes against salinity rather than distance is more appropriate in the case of the sandy terminus of a swash, it has proven inconclusive during our study. Substantial inputs of freshwater high in nutrients are possible throughout the length of the sand field and the resulting lack of a gradual salinity gradient is the most likely explanation. Future efforts should focus on locating, quantifying, and analyzing the nutrient concentrations of evident freshwater discharges and contrasting them with adjacent primary channel water and sediment and (swash zone) shore water. Moreover, the abundance of submerged aquatic macroalgae and feedback between them and nutrient inputs from surface discharges may prove to be useful indicators of the influence of the coastal terminus of swashes on the modification of land-derived nutrients before these nutrients reach the coastal ocean.

4.4. Channel Management

Migrating swash channels at the coastal sandy terminus amplify problems of erosion of private properties and may also prevent flushing of estuaries [22]. "Soft" remediation efforts may include realignment of the tidal channels and reconstruction of beach profiles during renourishment, while "hard" armored protection involves building solid-bottom culverts that would stabilize the tidal channel or constructing seawalls [42]. Construction of a concrete culvert would change one critical aspect of the primary channel: the surface area of the underlying substrate. Sediment provides a much higher surface area per unit volume (or per meter distance of a channel) than an impervious surface. Biofilms (and perhaps macroalgal mats) will inevitably form on the impervious surface and transform matter as it passes over them. Given our findings that show significant reservoirs of nutrients in sand, in the case of absence of the sandy substrate, those nutrients would otherwise have to be stored in hard-substrate epibiota or be exported to either side of the impervious culvert. Consideration must be given to the design of such a culvert and its potential impacts on the exchange of dissolved constituents between marsh and coastal ocean.

5. Conclusions

Our investigation focused on the sandy terminus of a marsh tidal creek, Singleton Swash, in Long Bay South Carolina. Sandy sediments in this terminus are highly permeable and characterized by DIN, PO_4^{3-}, and Chl *a* concentrations that are higher than those in the overlying water on most occasions, a pattern consistent with the role of coastal sediments as a major site of organic matter degradation, nutrient regeneration, and benthic primary productivity. Patterns in oxygen, nutrient,

and chlorophyll concentrations have a strong seasonal component and are explained by a shift in the photosynthesis–respiration balance between summer and winter. This pattern breaks down in April 2019 when substantial surface freshwater discharges, rich in nutrients, were observed from nearby developments concurrently with significant submerged aquatic macroalgal growth. The lack of a gradual salinity gradient from land to ocean in the primary channel of the sandy swash is in part due to significant flood currents that mix the marsh creek water mass and potentially substantial inputs of freshwater at the sandy terminus itself, thus rendering the application of a conservative mixing model on data from a given date only moderately informative. Future studies should focus on freshwater discharges and how their chemistry compares with immediately adjacent channel water and shore (ocean) water, as well as sedimentary indicators of primary productivity, such as the sedimentary (microphytobenthic) chlorophyll content and submerged aquatic macroalgal coverage. Given the importance and prominence of both benthic primary production indicators in our study, channel management measures that substantially modify the presence of a highly permeable substrate must be taken with the awareness that nutrient processing by substrate producers may be affected and impact the release of land-derived nutrients to the coastal ocean.

Author Contributions: A.K.H. and N.A.L. conceived and designed the study; N.A.L. and B.T.H. performed field observations, laboratory analyses, and data processing, with the supervision and contribution of A.K.H., and compiled internal thesis reports based on their work; the original draft of the manuscript was compiled by A.K.H. and was modified and edited by all authors. All authors have read and agreed to the published version of the manuscript.

Conflicts of Interest: The authors declare no conflict of interest. The funders had no role in the design of the study; in the collection, analyses, or interpretation of data; in the writing of the manuscript, or in the decision to publish the results.

References

1. NOAA. *National Coastal Population Report: Population Trends from 1970 to 2020*; National Oceanic and Atmospheric Administration: Silver Spring, MD, USA, 2013; p. 19.
2. Arnold, C.L.; Gibbons, C.J. Impervious Surface Coverage: The emergence of a key environmental indicator. *J. Am. Plan. Assoc.* **1996**, *62*, 243–258. [CrossRef]
3. Howarth, R.; Chan, F.; Conley, D.J.; Garnier, J.; Doney, S.C.; Marino, R.; Billen, G. Coupled biogeochemical cycles: Eutrophication and hypoxia in temperate estuaries and coastal marine ecosystems. *Front. Ecol. Environ.* **2011**, *9*, 18–26. [CrossRef]
4. Holland, A.F.; Sanger, D.M.; Gawle, C.P.; Lerberg, S.B.; Santiago, M.S.; Riekerk, G.H.M.; Zimmerman, L.E.; Scott, G.I. Linkages between tidal creek ecosystems and the landscape and demographic attributes of their watersheds. *J. Exp. Mar. Biol. Ecol.* **2004**, *298*, 151–178. [CrossRef]
5. Smith, E.; Sanger, D. *Determining the Role of Estuarine Swashes on Water Quality Impairment along the Grand Strand of South Carolina: Impacts of Land Use and Stormwater Runoff: A Final Report Submitted to the National Estuarine Research Reserve System Science Collaborative*; North Inlet-Winyah Bay NERR: Georgetown, SC, USA, 2015; p. 46.
6. Barnhardt, W.A. *Coastal Change along the Shore of Northeastern South Carolina—The South Carolina Coastal Erosion Study*; U.S.G.S. Circular 1339; U.S. Geological Survey: Reston, VA, USA, 2009; p. 77.
7. Hayes, M.O.; Michel, J. *A Coast for All Seasons: A Naturalist's Guide to the Coast of South Carolina*; Pandion Books: Columbia, SC, USA, 2008; p. 285.
8. Sanger, D.; Smith, E.; Voulgaris, G.; Koepfler, E.; Libes, S.; Riekerk, G.; Bergquist, D.; Greenfield, D.; Wren, P.; McCoy, C.; et al. Constrained enrichment contributes to hypoxia formation in Long Bay, South Carolina (USA), an open water urbanized coastline. *Mar. Ecol. Prog. Ser.* **2012**, *461*, 15–30. [CrossRef]

9. Webb, J.E.; Theodor, J. Irrigation of submerged marine sands through wave action. *Nature* **1968**, *220*, 682–683. [CrossRef]

10. Huettel, M.; Ziebis, W.; Forster, S.; Luther, G.W. Advective Transport Affecting Metal and Nutrient Distributions and Interfacial Fluxes in Permeable Sediments. *Geochim. Cosmochim. Acta* **1998**, *62*, 613–631. [CrossRef]

11. Boudreau, B.P.; Huettel, M.; Forster, S.; Jahnke, R.A.; McLachlan, A.; Middelburg, J.J.; Nielsen, P.; Sansone, F.; Taghon, G.; Van Raaphorst, W. Permeable marine sediments: Overturning an old paradigm. *Eos Trans. AGU* **2001**, *82*, 133–136.

12. Chipman, L.; Berg, P.; Huettel, M. Benthic oxygen fluxes measured by eddy covariance in permeable Gulf of Mexico shallow-water sands. *Aquat. Geochem.* **2016**, *22*, 529–554. [CrossRef]

13. Boulton, A.J.; Findlay, S.; Marmonier, P.; Stanley, E.H.; Valett, H.M. The functional significance of the hyporheic zone in streams and rivers. *Annu. Rev. Ecol. Evol. Syst.* **1998**, *29*, 59–81. [CrossRef]

14. Schutte, C.A.; Hunter, K.; McKay, P.; Di Iorio, D.; Joye, S.B.; Meile, C. Patterns and controls of nutrient concentrations in a Southeastern United States tidal creek. *Oceanography* **2013**, *26*, 132–139. [CrossRef]

15. Kim, K.H.; Heiss, J.W.; Michael, H.A.; Cai, W.-J.; Laattoe, T.; Post, V.E.A.; Ullman, W.J. Spatial patterns of groundwater biogeochemical reactivity in an intertidal beach aquifer: Beach aquifer biogeochemical reactivity. *JGR Biogeosci.* **2017**, *122*, 2548–2562. [CrossRef]

16. Berner, R.A. *Early Diagenesis: A Theoretical Approach*; Princeton University Press: Princeton, NJ, USA, 1980; p. 256.

17. Froelich, P.N.; Klinkhammer, G.P.; Bender, M.L.; Luedtke, N.A.; Heath, G.R.; Cullen, D.; Dauphin, P.; Hammond, D.; Hartman, B.; Maynard, V. Early oxidation of organic matter in pelagic sediments of the eastern equatorial Atlantic: Suboxic diagenesis. *Geochim. Cosmochim. Acta* **1979**, *43*, 1075–1090. [CrossRef]

18. MacIntyre, H.L.; Geider, R.J.; Miller, D.C. Microphytobenthos: The ecological role of the "Secret Garden" of unvegetated, shallow-water marine habitats. I. Distribution, abundance and primary production. *Estuaries* **1996**, *19*, 186. [CrossRef]

19. Anderson, I.C.; Brush, M.J.; Piehler, M.F.; Currin, C.A.; Stanhope, J.W.; Smyth, A.R.; Maxey, J.D.; Whitehead, M.L. Impacts of climate-related drivers on the benthic nutrient filter in a shallow photic estuary. *Estuar. Coast.* **2014**, *37*, 46–62. [CrossRef]

20. Pinckney, J.; Paerl, H.; Fitzpatrick, M. Impacts of seasonality and nutrients on microbial mat community structure and function. *Mar. Ecol. Prog. Ser.* **1995**, *123*, 207–216. [CrossRef]

21. USACE. *Singleton Swash Planning Assistance to States (PAS) Study*; U.S. Army Corps of Engineers: Charleston, SC, USA, 2009; p. 25.

22. Hoffnagle, B.L. Linking Water Quality and Beach Morphodynamics in a Heavily Impacted Tidal Creek in Myrtle Beach. Master's Thesis, Coastal Carolina University, Conway, SC, USA, 2015.

23. Pastore, D. Hydrodynamic Drivers of Dissolved Oxygen Variability within a Highly Developed Tidal Creek in Myrtle Beach. Master's Thesis, Coastal Carolina University, Conway, SC, USA, 2018.

24. Legut, N.A. The Role of a Permeable Sand Column in Modifying Tidal Creek Geochemistry and Land-Derived Inputs to the Coastal Ocean. Master's Thesis, Coastal Carolina University, Conway, SC, USA, 2019.

25. Pastore, D.M.; Peterson, R.N.; Fribance, D.B.; Viso, R.; Hackett, E.E. Hydrodynamic Drivers of Dissolved Oxygen Variability within a Tidal Creek in Myrtle Beach, South Carolina. *Water* **2019**, *11*, 1723. [CrossRef]

26. Klute, A.; Dirksen, C. *Hydraulic Conductivity and Diffusivity: Laboratory Methods*; Klute, A., Ed.; SSSA Book Series; American Society of Agronomy—Soil Science Society of America: Madison, WI, USA, 1986; pp. 687–734.

27. Rocha, C.; Forster, S.; Koning, E.; Epping, E. High-resolution permeability determination and two-dimensional porewater flow in sandy sediment: High-resolution permeability gradients in sands. *Limnol. Oceanogr. Methods* **2005**, *3*, 10–23. [CrossRef]

28. McManus, J. Grain Size Determination and Interpretation. In *Techniques, in Sedimentology*; Tucker, M., Ed.; Blackwell Scientific Publications: Oxford, UK, 1988; pp. 63–85.

29. Arar, E.J.; Collins, G.B. *Method 445.0—In Vitro Determination of Chlorophyll a and Pheophytin a in Marine and Freshwater Algae by Fluorescence*; U.S. Environmental Protection Agency: Washington, DC, USA, 1997; p. 23.

30. Hannides, A.K.; Glazer, B.T.; Sansone, F.J. Extraction and quantification of microphytobenthic Chl *a* within calcareous reef sands: Microphytobenthic Chlorophyll a in reef sands. *Limnol. Oceanogr. Methods* **2014**, *12*, 126–138. [CrossRef]

31. Santisteban, J.I.; Mediavilla, R.; López-Pamo, E.; Dabrio, C.J.; Blanca Ruiz Zapata, M.; José Gil García, M.; Martínez-Alfaro, P.E. Loss on ignition: A qualitative or quantitative method for organic matter and carbonate mineral content in sediments? *J. Paleolimnol.* **2004**, *32*, 287–299. [CrossRef]

32. Strickland, J.D.H.; Parsons, T.R. *A Practical Handbook of Seawater Analysis*, 2nd ed.; Fisheries Research Board of Canada: Ottawa, ON, Canada, 1972; p. 310.

33. Bendschneider, K.; Robinson, R.J. A new spectrophotometric method for the determination of nitrite in seawater. *J. Mar. Res.* **1952**, *11*, 87–96.

34. Holmes, R.M.; Aminot, A.; Kérouel, R.; Hooker, B.A.; Peterson, B.J. A simple and precise method for measuring ammonium in marine and freshwater ecosystems. *Can. J. Fish. Aquat. Sci.* **1999**, *56*, 1801–1808. [CrossRef]

35. Murphy, J.; Riley, J.P. A modified single solution method for the determination of phosphate in natural waters. *Anal. Chim. Acta* **1962**, *27*, 31–36. [CrossRef]

36. Hansen, H.P.; Koroleff, F. Determination of Nutrients. In *Methods of Seawater Analysis*; Grasshoff, K., Kremling, K., Ehrhardt, M., Eds.; Wiley-VCH Verlag GmbH: Weinheim, Germany, 1999; pp. 159–228.

37. Sokal, R.R.; Rohlf, F.J. *Biometry*, 3rd ed.; W.H. Freeman: New York, NY, USA, 1994; p. 880.

38. Wu, M.L.; Hong, Y.G.; Yin, J.P.; Dong, J.D.; Wang, Y.S. Evolution of the sink and source of dissolved inorganic nitrogen with salinity as a tracer during summer in the Pearl River Estuary. *Sci. Rep.* **2016**, *6*, 36638. [CrossRef] [PubMed]

39. Berg, P.; Røy, H.; Janssen, F.; Meyer, V.; Jørgensen, B.; Huettel, M.; de Beer, D. Oxygen uptake by aquatic sediments measured with a novel non-invasive eddy-correlation technique. *Mar. Ecol. Prog. Ser.* **2003**, *261*, 75–83. [CrossRef]

40. Underwood, G.J.C.; Paterson, D.M.; Parkes, R.J. The measurement of microbial carbohydrate exopolymers from intertidal sediments. *Limnol. Oceanogr.* **1995**, *40*, 1243–1253. [CrossRef]

41. Williams, T.M.; Hitchcock, D.; Song, B.; O'Halloran, T. Hurricane Florence flooding in Georgetown County: A qualitative explanation of the interactions of estuary and tidal river. *J. S. C. Water Resour.* **2019**, *6*, 36–45. [CrossRef]

42. United States Army Corps of Engineers (USACE) and The South Carolina Department of Health and Environmental Control (SCDHEC) Joint Public Notice Singleton Swash Stabilization (P/N # 2014-00013-3H). 2014, p. 14. Available online: https://www.sac.usace.army.mil/Portals/43/docs/regulatory/publicnotices/Jan14_PN/SAC-2014-00013-3H_Horry_County_Singleton_Swash_Stabilization.pdf?ver=2014-01-09-090033-390 (accessed on 20 May 2019).